Journal of Neuroscience Methods 279 (2017) 13–21

Contents lists available at ScienceDirect

Journal of Neuroscience Methods

journal homepage: www.elsevier.com/locate/jneumeth

Dendritic spine classification using shape and appearance features based on two-photon microscopy

Muhammad Usman Ghani[a,**], Fitsum Mesadi[b], Sümeyra Demir Kanık[a], Ali Özgür Argunşah[c,*], Anna Felicity Hobbiss[c], Inbal Israely[c,1], Devrim Ünay[d], Tolga Taşdizen[b], Müjdat Çetin[a]

[a] Signal Processing and Information Systems Lab., Faculty of Engineering and Natural Sciences, Sabanci University, Istanbul, Turkey
[b] Electrical and Computer Engineering Department, University of Utah, Salt Lake City, UT, USA
[c] Champalimaud Neuroscience Programme, Champalimaud Centre for the Unknown, Lisbon, Portugal
[d] Biomedical Engineering Department, Faculty of Engineering, Izmir University of Economics, Izmir, Turkey

HIGHLIGHTS

- A statistical machine learning-based spine classification approach is proposed.
- Our classification framework enables to study the separability of spine shape classes.
- Proposed approach outperforms state-of-the-art morphological feature based methods.
- A fully annotated dataset of 2PLSM images of three types of spines will be released.

ARTICLE INFO

Article history:
Received 27 August 2016
Received in revised form 9 December 2016
Accepted 13 December 2016
Available online 18 December 2016

Keywords:
Dendritic spines
Classification
Disjunctive Normal Shape Model
Histogram of oriented gradients
Shape analysis
Kernel density estimation
Microscopy

ABSTRACT

Background: Neuronal morphology and function are highly coupled. In particular, dendritic spine morphology is strongly governed by the incoming neuronal activity. The first step towards understanding the structure-function relationships is to classify spine shapes into the main spine types suggested in the literature. Due to the lack of reliable automated analysis tools, classification is mostly performed manually, which is a time-intensive task and prone to subjectivity.
New method: We propose an automated method to classify dendritic spines using shape and appearance features based on challenging two-photon laser scanning microscopy (2PLSM) data. Disjunctive Normal Shape Models (DNSM) is a recently proposed parametric shape representation. We perform segmentation of spine images by applying DNSM and use the resulting representation as shape features. Furthermore, we use Histogram of oriented gradients (HOG) to extract appearance features. In this context, we propose a kernel density estimation (KDE) based framework for dendritic spine classification, which uses these shape and appearance features.
Results: Our shape and appearance features based approach combined with Neural Network (NN) correctly classifies 87.06% of spines on a dataset of 456 spines.
Comparison with existing methods: Our proposed method outperforms standard morphological feature based approaches. Our KDE based framework also enables neuroscientists to analyze the separability of spine shape classes in the likelihood ratio space, which leads to further insights about nature of the spine shape analysis problem.
Conclusions: Results validate that performance of our proposed approach is comparable to a human expert. It also enable neuroscientists to study shape statistics in the likelihood ratio space.

* Corresponding author. Present address: Brain Research Institute, University of Zurich, Zurich, Switzerland. Phone: +41784011868.
** Corresponding author. Present address: Department of Electrical and Computer Engineering – Boston University, Boston, MA, USA. Phone: +18577538589.
E-mail addresses: mughani@bu.edu (M.U. Ghani), argunsah@hifo.uzh.ch (A.Ö. Argunşah), ii2176@cumc.columbia.edu (I. Israely).
[1] Present address: Department of Pathology and Cell Biology, College of Physicians and Surgeons, Columbia University, New York, NY, USA.

http://dx.doi.org/10.1016/j.jneumeth.2016.12.006
0165-0270/

1. Introduction

Dendritic spines are the post-synaptic partners of synapses and their morphology is highly coupled with the activity they are subjected to Bartol et al. (2015), Lippman and Dunaevsky (2005), Yuste (2010, 2001), Matsuzaki et al. (2004), Harvey and Svoboda (2007), Govindarajan et al. (2011), Shi et al. (2009). Synapses are proposed to be the sites where memories stored through activity-dependent potentiation and depression mechanisms (Whitlock et al., 2006). Spine morphology and density are altered in diseases such as Alzheimer's disease and Parkinson's disease (Son et al., 2011; Xu and Wong, 2006).

A dendritic branch with several spines captured using two-photon laser scanning microscopy (2PLSM) is shown in Fig. 1. Each dendritic spine has a small bulbous head that is connected to the parent dendritic shaft through a narrow neck (Koh et al., 2002). The morphological properties of spine neck and head are usually not proportional to each other, nor are the spine neck diameter and neck length related (Yuste, 2010). Spines have been known to show extraordinary diversity (Ruszczycki et al., 2012). They are reported to have different densities and sizes across different brain areas, cell types, and animal species (Yuste, 2010). Even within a particular cell, spines exhibit a great variety of spine neck and head dimensions (Yuste, 2010). Spines compartmentalize electrical and biochemical processes that modulate the level of interactions at synapses (Tonnesen et al., 2014). Spine neck length is reported to be proportional to its functional properties (Arellano et al., 2007), since its impedance enables filtering of membrane electrical potentials (Yuste, 2010; Arellano et al., 2007) and neck diameter and length are also reported to affect the diffusional coupling between spine and dendrite (Rodriguez et al., 2008; Harris, 1999). Additionally, postsynaptic density (PSD) area is found to be correlated with spine head diameter and the number of postsynaptic receptors (Yuste, 2010; Arellano et al., 2007).

Dendritic spines have different shape types, and it has been proposed that these different morphological variations could be related to various functional roles or developmental stages (Parnass et al., 2000). Traditionally, dendritic spines are grouped into four classes: mushroom, stubby, thin, and filopodia (Yuste, 2010; Son et al., 2011; Rodriguez et al., 2008; Chang and Greenough, 1984; Peters and Kaiserman-Abramof, 1970). An example image of each of these classes is given in Fig. 2. Mushroom spines have large bulbous heads and long necks, thin spines have small heads and thin long necks, whereas the neck in stubby spines is either missing or very small, and filopodia are found to have longer necks and generally do not have clear heads (Yuste, 2010). As discussed earlier, the distribution of different types of spines varies in different parts of brain. This is also dependent upon the age. For instance stubby spines are known to be dominant during early postnatal development but they are found in adult animals as well (Yuste, 2010).

Quantitative analysis of dendritic spines is important for neurobiological research as it may help researchers understand the underlying structure to function relationship. Currently this analysis is mostly performed manually due to the unavailability of reliable automated analysis tools. Such tools would accelerate research in this domain and help neuroscientists understand the relationship between neuronal activity and morphological changes in spines.

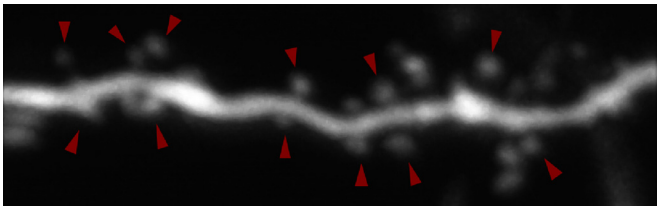

Fig. 1. A dendritic branch with several spines imaged using a two-photon laser scanning microscope (2PLSM) is shown, arrows point at some of the spines attached to the dendritic branch.

Rodriguez et al. (2008) conducted a study on spine classification based on 3D images acquired by confocal laser scanning microscopy (CLSM) and computed head to neck ratio, neck length, head diameter, and aspect ratio. They performed classification using a decision tree and used manual labels assigned by human expert operators to validate the performance of their approach. They reported intra-operator and inter-operator variability while assigning the labels. Son et al. (2011) used neck diameter, head diameter, shape criteria, area, length, and perimeter with a decision tree to classify spines. They also used CLSM for imaging and human expert assigned labels for evaluation. Shi et al. (2009) developed a semi-supervised learning approach based on 3D images acquired using CLSM and used a weighted feature set consisting of neck diameter, head diameter, volume, and length for classification of spines. A recent study on spine classification based on CLSM images extracted morphological features and used a rule-based classification approach (Basu et al., 2016).

Koh et al. (2002) developed a classification approach based on ratio criteria inspired by Harris et al. (1992) using the ratio of spine length to neck diameter, and ratio of head diameter to neck diameter. They used 2PLSM to acquire images. A recent spine analysis study based on 2PLSM images (Ghani et al., 2015) considered head diameter, neck length, perimeter, area and other morphological features to classify spines as either mushroom or stubby types. Head diameter and neck length were described to be the most important features, which was later supported by another study (Ghani et al., 2016) where ISOMAP (Tenenbaum et al., 2000) has been applied to compute the two most prominent features on a 2PLSM spine data-set. Erdil et al. (2015) applied intensity based features to perform classification of spines from 2PLSM intensity images.

Most of the studies on spine analysis focus on CLSM image, however, there are only a few studies that considered 2PLSM images. Another observation is that most of the studies considered morphological features and rule based classifiers. This research attempts to fill this gap and propose a shape and appearance features based classification technique.

This study is based on 2PLSM images. Analyzing 2PLSM images is more challenging in comparison to confocal laser scanning microscopy (CLSM) images due to lower signal to noise characteristics. Additionally, following the Abbe's law (Lipson et al., 2010), the resolution of 2PLSM images is half of the CLSM images. However, 2PLSM has the capability to image living cells with a reduced toxicity than CLSM thus can produce dynamic data, which would capture shape transitions during synaptic process, allowing the analysis of tissues over time (Koh et al., 2002; So et al., 2000). This is possible because 2PLSM causes reduced photo-damage and bleaching, two of the major limitations of fluorescence microscopy of living tissues and cell, due to a much smaller point of excitation than CLSM (So et al., 2000). Experiments with 2PLSM therefore permit the imaging of cells over prolonged periods of time, which produces large volumes of data. Neuroscientists studying the structure–function relationships use the 2PLSM and perform analysis manually, which is more challenging due to the low resolution, low SNR, and large amount of data. The techniques proposed in this paper would be of interest to neuroscientists interested in analyzing large volumes of such temporal data. This would accelerate the analysis process and would possibly assist neuroscientists to understand the structure–function relationships.

We propose an automated dendritic spine shape analysis framework in this paper. Disjunctive Normal Shape Models (DNSM) is a recently proposed shape model; we exploit its parametric nature

(a) Intensity images collected using 2PLSM

(b) Manual annotations

Fig. 2. Spine classes: mushroom, stubby, thin, filopodia (left to right). Intensity and corresponding manually annotated images are shown for each shape class.

and use it as a feature extraction approach. DNSM (Ramesh et al., 2015) is an implicit model that represents a shape through the union of convex polytopes that are constructed by intersections of half spaces. Mesadi et al. (2015) introduced DNSM-based shape and appearance priors and tested their potential on various segmentation problems. This approach has proven successful, because it provides better segmentation as compared to the existing state-of-the-art approaches. We apply this approach to segment the dendritic spines from maximum intensity projected (MIP) (Wallis et al., 1989) images and use its parameters as shape features.

Further, our analysis of 2PLSM images has also suggested that the intensity distribution inside spines also contains some information which could be useful for classification. However, we also noticed that intensity level varies across dendritic branches and datasets, which suggests using gradients rather than absolute intensity information. Histogram of oriented gradients (HOG) (Dalal and Triggs, 2005), as the name suggests, computes histograms of gradient directions and applies contrast normalization. HOG has been widely used for object detection and recognition tasks in computer vision. Therefore, we decided to apply HOG to compute appearance features.

As we will discuss later in this paper, the spine classes have overlapping distributions, which makes the spine classification problem challenging. To perform classification, we propose and use a kernel density estimation (KDE) based approach. This non-parametric approach intrinsically provides the likelihood of membership for each spine class in a principled manner. In order to evaluate the performance of developed approach, the output of the classification algorithm is compared to the labels assigned by a neuroscience expert. The achieved results validate that performance of the proposed approach is comparable to a neuroscience expert.

The idea of classifying spines into distinct classes has been used in many studies, however, there is still an open question on whether distinct spine classes exist or whether these should be modeled through a continuum of shape variations. Studies reported in Arellano et al. (2007), Peters and Kaiserman-Abramof (1970), Ghani et al. (2016) pointed that some spines in their dataset had intermediate shapes and were difficult to assign to one of the standard classes. Spacek and Hartmann (1983) additionally added two intermediate spine classes between stubby, and mushroom; and mushroom, and thin spines. Wallace and Bear (2004) claimed that morphological measurements of spines acquired from their data do not support the idea of existence of distinct spine classes. Ruszczycki et al. (2012) believe that there is no standard classification rule, and different researchers may use different criteria. We have also noted similar observations in the literature that there is no standard for classification and that each group defines the classes based on single or multiple expert/experts they work with, which causes analysis results to suffer from subjectivity. There seems to be a lack of a standard dataset publicly available for research. We will make the dataset used in this paper publicly available including raw data, manual annotations, and manual labels.[2]

Thanks to the nonparametric statistical structure of our KDE-based approach, it has the potential to represent complicated shape distributions well. Additionally, it provides a simplified framework that enables us to examine the shape distributions, including the question of whether the spine shapes constitute a continuum across classes.

The major contributions of this paper are; use of the DNSM based implicit parametric shape representation for feature extraction, the use of HOG to extract appearance features, the development of a KDE based spine shape classification approach, and a fully annotated dataset of 2PLSM images of three types of spines. Exploring the separability of spine shape classes in likelihood ratio space is another contribution of this paper. To the best of our knowledge, this is the first fully automated statistical machine learning-based approach for classification of spines from 2PLSM data with an extensive evaluation. Although we demonstrate the usefulness of our proposed approach on 2PLSM data, the proposed approach can be applied to spine data acquired with other imaging modalities as well.

The rest of this paper is organized as follows: an overview of image acquisition process is presented in Section 2. Detailed methodology of our proposed approach is described in Section 3. Experimental results are discussed in Section 4. Section 5 presents the conclusion of this study and future work suggestions.

2. Image acquisition

In order to be imaged under 2PLSM, hippocampal neurons from mouse organotypic slice cultures postnatal day 7–10 were transfected using biolistic gene transfer with gold beads (10 mg, 1.6 μm diameter, Biorad) coated with Dendra-2 (Evrogen) plasmid DNA (100 μg) or AFP using a Biorad Helios gene gun after 4 or 7 days in vitro.[3]

Imaging experiments were performed 2–5 days post-transfection. Slices were perfused with artificial cerebrospinal fluid (ACSF) containing 127 mM NaCl, 2.5 mM KCl, 25 mM $NaHCO_3$, 1.25 mM NaH_2PO_4, 25 mM D-glucose, 2 mM $CaCl_2$ and 1 mM $MgCl_2$ (equilibrated with O_2 95%, CO_2 5%) at room temperature at a rate of 1.5 ml/min. Two-photon imaging was performed using a galvanometer-based scanning system (Prairie Technologies, acquired by Bruker Inc.) on an Olympus BX61WI equipped with 60X water immersion objective (0.9 NA), using a Ti:sapphire laser (Coherent Inc.) controlled by PrairieView software at 910 nm. Z-stacks (0.3 μm axial spacing) from secondary or tertiary dendrites from CA1 neurons were collected every 5 min for up to 4 h. The field of view was 19.8 × 19.8 μm at 1024 × 1024 pixels.

3. Methods

A preliminary version of this work has been reported in (Ghani et al., 2016). That study only involved shape-based analysis of two

[2] https://github.com/mughanibu/Dendritic-Spine-Analysis-Dataset.

[3] All animal experiments are carried out in accordance with European Union regulations on animal care and use, and with the approval of the Portuguese Veterinary Authority (DGV).

spine classes on a limited dataset, whereas this paper presents an approach for joint shape and appearance-based classification of three spine types on an extended dataset. Section 3.1 explains the pre-processing procedures applied in this study, Section 3.2 describes the process for computing DNSM-based shape features, Section 3.3 provides the details of HOG-based appearance feature extraction process, Section 3.4 describes the feature selection techniques applied, and Section 3.5 presents the details of KDE based classification framework.

3.1. Pre-processing

We acquired 3D stacks of 40 dendritic branches. We projected the 3D images to 2D using MIP and applied median filtering to reduce noise. The ground truth for segmentation and classification were prepared by an expert from 2D images. We selected 456 dendritic spines consisting of 288 mushroom, 113 stubby, and 55 thin spines. The technique described in Section 3.2 is applied to segment spines in this study, which requires the input images to be aligned. Firstly, we choose a region of interest (ROI) in the projected 2*D* image for each spine. The ROI is selected in a way that spine head center is placed approximately at the center of the ROI. Further, each spine image is scaled to 250×250 pixels. In order to keep the aspect ratio same (so that scaling does not affect the shape), the selected ROI is always square. Finally, we rotate each spine image such that spine neck is perpendicular to horizontal axis. This process currently involves manual procedures. However, the process can be automated by applying Hough Circle Transform (Atherton and Kerbyson, 1999) to locate the spine head center and by computing the spine neck path to detect its orientation with respect to the dendrite surface (Ghani et al., 2015).

3.2. DNSM-based feature extraction

Shapes can be represented using a characteristic function, and DNSM approximates shape characteristic function by a union of N convex polytopes. These polytopes are constructed by intersection of M half-spaces. The resulting DNSM approximation to the characteristic function of shape is presented in Eq. (1).

$$f(\mathbf{x}) = 1 - \prod_{i=1}^{N} \left(1 - \prod_{j=1}^{M} \frac{1}{1 + e^{\sum_{k=1}^{D+1} w_{ijk} x_k}} \right) \tag{1}$$

where, $\mathbf{x} = \{x, y, 1\}$, and $D = 2$ for 2-dimensional (2D) shapes. w_{ijk} are the only free parameters in DNSM and they determine the position and orientation of half-spaces (discriminants). We use MIP (2D) images in this work, however, the DNSM approach is generic and can be straightforwardly extended to 3*D* shapes. For further details of DNSM, readers are referred to (Ramesh et al., 2015).

On top of the basic DNSM shape representation, Mesadi et al. (2015) introduced DNSM based shape and appearance priors to improve segmentation. In this paper, we apply this DNSM based approach to segment dendritic spines. This approach exploits the parametric nature of DNSM, and learns shape and appearance features from training data to segment test images. DNSM shape and appearance priors based approach has two stages for the segmentation of spines: training, and testing. For this purpose, we divided our data into training and testing sets using a 10 fold cross validation procedure.

The training stage consists of two steps. The first is to represent the manually segmented (binary) spine image using DNSM parameters. During the second step, we construct local appearance and shape priors from training intensity and binary images. Due to the parametric nature of DNSM, we can construct shape priors at shape, polytope, and half-space levels. The use of local priors would move the shape towards locally similar training samples during the testing stage. Local shape priors are constructed by linearly combining the polytope training shapes. This method generates an ample amount of shape variations by local combinations of training shapes, which enables this method to produce good segmentation results even with limited training data. Local appearance priors are constructed by first assigning each pixel to its nearest half-space, and then building two histograms for each half-space: one for background and other for foreground pixels. These local appearance priors constructed by intensity statistics around each half-plane equip this method with better expressive capability to represent the training data. The use of local appearance priors is especially important for spine segmentation, since spine segmentation requires distinguishing between dendrite and spine regions. As intensity levels for spine and dendrite regions are similar in 2PLSM images, it becomes crucial to use local appearance priors in order to provide good spine segmentation.

Spines are segmented in the testing stage by minimizing the weighted average of appearance and shape energy terms. Here the appearance energy term uses the intensity data. Weights w_{ijk} are updated in each iteration using gradient descent, as illustrated in Eq. (2).

$$w_{ijk} \leftarrow w_{ijk} - \alpha \frac{\partial E_{Shape}}{\partial w_{ijk}} - \gamma \frac{\partial E_{Appr}}{\partial w_{ijk}} \tag{2}$$

where α, and γ are the levels of contributions from shape and appearance terms in updating the weights, w_{ijk}.

This approach has several parameters which must be tuned for different applications: number of half spaces M, number of polytopes N; and level of contribution from shape priors α, and appearance priors γ. We used the same values for these parameters as suggested by Ghani et al. (2016): $M = 16$, $N = 8$, $\alpha = 0.05$, and $\gamma = 0.5$. Segmentation results for a few spines are given in Fig. 3. As a result of segmentation, we have achieved the approximated form of the characteristic function of each spine shape in terms of DNSM parameters. The DNSM represents each segmented image using $M \times N \times 3$ parameters. As discussed earlier, in this paper we exploit DNSM's parametric nature and use DNSM parameters as feature vectors to train the classifier to perform spine classification. We also use this feature space to study shape statistics.

3.3. Appearance feature computation

HOG (Dalal and Triggs, 2005) characterizes the local appearance features by computing 1D histograms of gradient orientations. HOG has been studied extensively in the literature and has been successful in various object detection and recognition tasks. We observed in our data that spines have uniform intensities inside the head, however, this is not true for the neck. A decreasing intensity pattern can be noticed in the neck part of spines. This is useful information since stubby spines have short heads and no or short necks, mushroom spines have big heads and long necks, and thin spines have small heads and long necks. Hence using this local appearance information would assist us in the spine classification task.

The HOG representation is achieved in several steps. The first step involves dividing the image into small spatial regions called "cells" and computing gradient orientations in each cell. Then the gradient orientations are divided into smaller regions called "bins". A 1D histogram is constructed for each bin by accumulating the corresponding gradient directions. Further, Dalal and Triggs (2005) suggested applying contrast normalization in order to achieve illumination invariance properties for achieved descriptors. Contrast normalization is applied using relatively large regions called "blocks" and normalizing the cell histograms by block histograms. Overlapping blocks are used for sufficient contrast normalization.

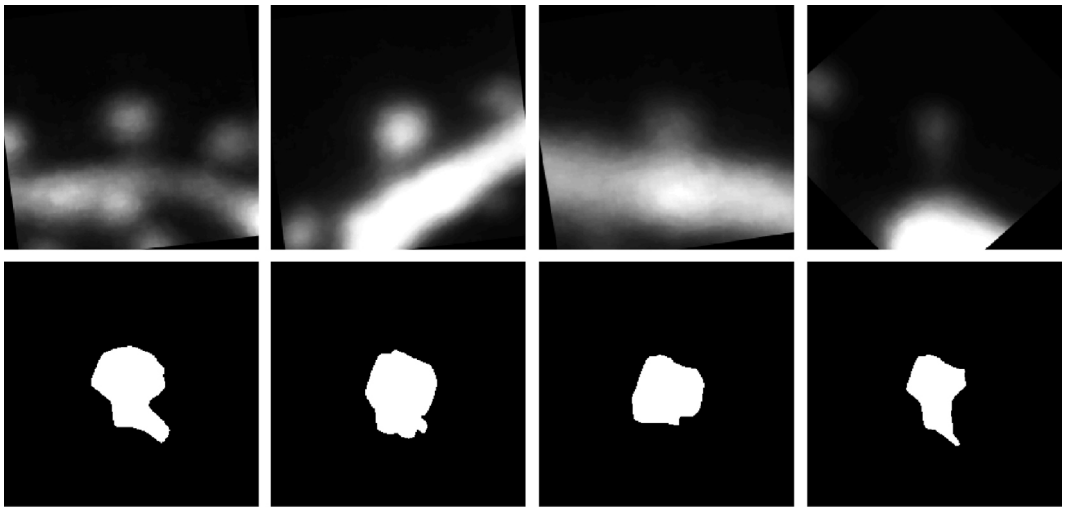

Fig. 3. A few images from dataset, without segmentation (above) and segmented images (below). The first 2 spines are labeled as mushroom, the 3rd spine as stubby, and the 4th as thin. Spines are segmented using DNSM shape and appearance priors based approach (Mesadi et al., 2015). Automated segmentation results are not perfect; sometimes suffering from over-segmentation and in some cases under-segmentation. But these segmentation results fairly represent the shape types and can be used for classification.

The final step involves constructing a single 1D descriptor by combining all the histograms.

In order to compute HOG features, we select a region of interest (ROI) in intensity images such that the spine is completely inside the ROI and it does not include parts of dendrite. This does not require ROIs for all spines to have the same dimensions. We rotate the ROIs such that spine necks are vertically aligned. Several images from this dataset are shown in Fig. 4. The reason behind selecting a separate ROI for HOG features is to remove the dendritic branch and reduce other artifacts.

As discussed earlier, HOG has different components and changing their values affect the descriptors. These parameters include: cell size, block size, block overlap ratio, and number of oriented histogram bins. The choice for the value of cell size depends upon whether we are interested in global/large-scale features or local features. If we are interested in large-scale features, a large cell size value would be desired. Increasing the cell size will capture more pixels, this as a result we will lose local level or small scale changes and will only be able to keep global information. Similar to cell size, a small block size will allow us to keep track of local illumination changes. If we want to perform contrast normalization, a block size value greater than cell size would be required. Contrast normalization is also controlled through block overlap, the number of overlapping cells in adjacent blocks. If we use unsigned gradient directions, we cannot differentiate between dark to light, and light to dark intensity transitions. The number of histogram orientation bins controls the size of the feature vector. A large value increases the feature vector size but enables capturing finer intensity changes. We performed experiments with different values of HOG features and empirically selected the values of HOG parameters to be, $CellSize = [height/5, width/5]$, $BlockSize = 2 \times CellSize$, $BlockOverlap = 1$, and $Bins = 9$.

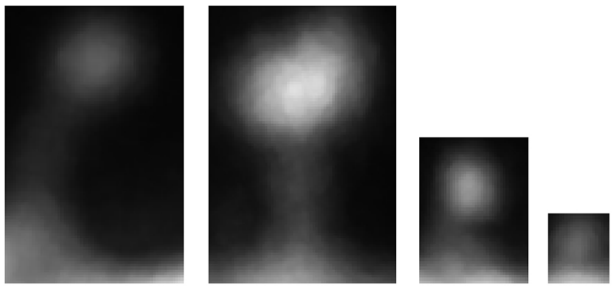

Fig. 4. Sample images from dataset prepared for HOG feature extraction. The first spine is labeled as thin, 2nd and 3rd as mushroom, and 4th as stubby (from left to right).

3.4. Feature selection

Our shape based feature extraction process produces a 384-dimensional feature vector, whereas the appearance based feature extraction process produces a 576-dimensional feature vector. As we are considering a 3 class problem here, some of the features might be redundant or less relevant for classification. Hence it would be of interest to apply some feature selection techniques and perform classification on reduced-dimensional features. We consider two feature selection techniques: (i) correlation based feature selection (CFS) (Hall, 1999), and (ii) information gain based feature selection (IG) (Cover and Thomas, 1991). CFS selects features based on their correlation and intercorrelation scores to different classes. IG weights features based on information gain with respect to a class and produces a score for each feature, we select the features with score of 0.1 and greater.

3.5. KDE based Classification

We estimate non-parametric density functions of class-conditional features using kernel density estimation (KDE) and apply likelihood ratio tests (LRT) to perform classification. In this work, we use KDE and LRT for analysis of 2*D* MIP images of spines, however, KDE and LRT are generic in nature and could potentially be applied to an arbitrary dimensional dataset. Our non-parametric density estimation approach is similar to Kim et al. (2007). Assuming we have m data samples: $x_1, x_2, \ldots, x_m$, having the n-dimensional density function $p(x)$, the Parzen density can be estimated by applying Eq. (3).

$$\hat{p}(x) = \frac{1}{m}\sum_{i=1}^{m} k(x - x_i, \Sigma) \tag{3}$$

where, $k(x, \Sigma) = \mathcal{N}(x; 0, \Sigma^T\Sigma)$ is an n-dimensional kernel, which can be simplified using the assumption that the kernel is spherical,

i.e., $\Sigma = \sigma I$. Applying this assumption, Eq. (3) can be simplified, as follows:

$$\hat{p}(x) = \frac{1}{m}\sum_{i=1}^{m} k(d(x, x_i), \sigma), \tag{4}$$

where $d(x, x_i)$ is the ℓ_2 distance between x and x_i in $\mathbb{R}^n$ and $k(x, \sigma) = \mathcal{N}(x; 0, \sigma^2)$ is the 1D Gaussian kernel. Kernel size (σ) is estimated by the bracket method (also known as the bisection method) (Richard and Burden, 1988). First, we compute 1D kernel size from each feature and use this n dimensional kernel size vector to compute minimum (σ_{min}) and maximum kernel size (σ_{max}). Secondly, we apply the bracket method to compute the maximum likelihood kernel size in $[\sigma_{min}, \sigma_{max}]$ range by iteratively bisecting the interval and selecting the subinterval that contains the optimal kernel size. We compute three nonparametric density estimates for the three spine classes based on training data in each class: $\hat{p}_m(x)$, $\hat{p}_s(x)$, and $\hat{p}_t(x)$.

Once we have estimated the nonparametric density estimates for each class, the likelihood of an image belonging to Mushroom (l_m), Stubby (l_s), and Thin (l_t) classes can be estimated as follows:

$$\begin{aligned} l_m(x^{obs}) &= \hat{p}_m(x = x^{obs}), \\ l_s(x^{obs}) &= \hat{p}_s(x = x^{obs}), \\ l_t(x^{obs}) &= \hat{p}_t(x = x^{obs}), \end{aligned} \tag{5}$$

After estimating the likelihood for each class, we can perform classification using the LRT. This is a 3-class problem and requires multiple likelihood comparisons; we define 2 likelihood ratios, as depicted in Eq. (6), where $\mathcal{L}_s$ stands for stubby and $\mathcal{L}_t$ for thin spines.

$$\begin{aligned} \mathcal{L}_s &= \frac{l_s}{l_m} \\ \mathcal{L}_t &= \frac{l_t}{l_m} \end{aligned} \tag{6}$$

Finally, we can compare these likelihood ratios to perform classification:

$$\mathcal{L}_s \underset{\text{Not S}}{\overset{\text{Not M}}{\gtrless}} 1 \tag{7}$$

$$\mathcal{L}_s \underset{\text{Not S}}{\overset{\text{Not T}}{\gtrless}} \mathcal{L}_t \tag{8}$$

$$\mathcal{L}_t \underset{\text{Not T}}{\overset{\text{Not M}}{\gtrless}} 1 \tag{9}$$

Here "Not M" means do not decide mushroom as the classification decision, "Not S" means do not decide stubby, and "Not T" means do not decide thin as classification decision. In this manner we use an elimination procedure until we are left with only one possible class that is used as the decision. This approach simplifies the classification process by mapping an n-dimensional classification problem to a 2D problem, specifying the problem in terms of likelihood ratios which constitute the sufficient statistics for the classification problem. Fig. 5 illustrates the decision regions for classification in the 2D likelihood ratio space.

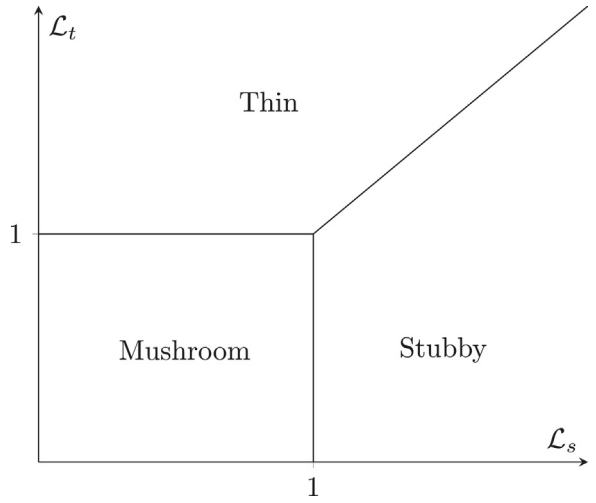

Fig. 5. Decision regions for classification in 2D likelihood ratio space.

4. Results and discussion

We extract shape and appearance based features and perform classification. In order to evaluate the classification results, we use labels assigned by a human expert. We compare classification results of our approach to four morphological feature based approaches: Ghani et al. (2015), Koh et al. (2002), NeuronStudio (Rodriguez et al., 2008), and 2dSpAn (Basu et al., 2016). NeuronStudio uses an automated spine detection algorithm; their approach misses 83 of the spines from our complete dataset. 2dSpAn uses a global thresholding based approach for dendrite and spine segmentation (using different threshold for each image), and fails to segment 197 of the spines from our complete dataset. For fair comparison, we present results on three datasets; DatasetA: complete dataset, DatasetB: which includes only the spines that are successfully detected by the NeuronStudio spine detection algorithm, and DatasetC: which includes only the spine that are segmented by the 2dSpAn segmentation approach. DatasetA consists of 456 spines including 288 mushroom, 113 stubby, and 55 thin type spines. DatasetB consists of 373 spines including 251 mushroom, 96 stubby, and 26 thin type spines. DatasetC consists of 259 spines including 182 mushroom, 71 stubby, and 6 thin spines.

Koh et al. (2002) extracted morphological features and performed classification using ratio criteria. However, these criteria seem to be very specialized for specific data with the result that their performance is very poor on our dataset, as shown in Table 1. In order to test the potential of their proposed features, we trained KDE, SVM, and NN, and performed classification using the same settings used for other methods. This performance is closer to other morphological features based approaches, which means that ratio criterion based classification approach is very specialized to some datasets and it must be used cautiously.

In order to perform the comparison with NeuronStudio (Rodriguez et al., 2008), we downloaded the latest (0.9.92) version of NeuronStudio[4] and computed classification results. After loading and setting dataset parameters, we used semi-automatic dendrite tracing by providing a manual seed. After dendrite tracing, we used NeuronStudio's built-in spine detection and classification tools to compute classification results on DatasetB. Although Neuronstudio uses 3D data for analysis, its performance is even worse than our morphological features based approach (Ghani et al., 2015) that only relies on 2D data. Additionally, our shape and appearance features based approach outperforms Neuronstudio with a margin of more than 20%. Neuronstudio's performance suffers from its morphology based features and rule based classification process.

2dSpAn (Basu et al., 2016) is a recently developed tool for spine classification. Initially, the user clicks on two points in the image to select the ROI. It uses global thresholding to perform segmentation. The threshold can be manually adjusted. However,

[4] http://research.mssm.edu/cnic/tools-ns.html.

Table 1
Results of classification of three spine types. Joint and separate use of the proposed KDE classification method and shape (DNSM) and appearance-based (HOG) feature extraction methods are evaluated and compared with existing spine classification methods of Koh et al. (2002), Rodriguez et al. (2008), Basu et al. (2016), Ghani et al. (2015) as well as other state-of-the-art classifiers one might consider.

Classifier	Features	DatasetA	DatasetB	DatasetC
KDE	Ghani et al. (2015)	61.18%	61.39%	64.87%
	Koh et al. (2002)	54.17%	54.16%	52.12%
	DNSM (Ghani et al., 2016)	75.60%	75.34%	75.29%
	HOG	83.11%	84.45%	**86.87%**
	DNSM + HOG	82.02%	83.65%	84.94%
	DNSM + HOG + CFS	**84.87%**	85.26%	87.26%
	DNSM + HOG + IG	83.33%	**85.79%**	85.71%
SVM	Ghani et al. (2015)	69.30%	75.60%	74.13%
	Koh et al. (2002)	69.52%	72.92%	76.06%
	DNSM (Ghani et al., 2016)	74.12%	78.82%	74.90%
	HOG	**82.46%**	82.04%	85.71%
	DNSM + HOG	81.36%	**82.57%**	**86.10%**
	DNSM + HOG + CFS	80.48%	81.50%	84.94%
	DNSM + HOG + IG	79.83%	81.77%	85.33%
NN	Ghani et al. (2015)	69.96%	71.31%	74.90%
	Koh et al. (2002)	67.54%	70.78%	72.97%
	DNSM (Ghani et al., 2016)	80.70%	82.04%	84.94%
	HOG	84.21%	84.72%	**87.26%**
	DNSM + HOG	85.53%	84.97%	85.33%
	DNSM + HOG + CFS	83.55%	86.33%	86.10%
	DNSM + HOG + IG	**87.06%**	**87.13%**	86.87%
Ratio criteria	Koh et al. (2002)	25.66%	26.27%	19.04%
NeuronStudio (Rodriguez et al., 2008)		–	60.86%	–
2dSpAn (Basu et al., 2016)		–	–	39.38%

Results presented as bold face represent best performance of a classifier on a Dataset.

due to the challenging nature of 2PLSM data it is hard to segment all the spines using a global threshold. Therefore, we select the threshold manually for each image so that the maximum number of spines can be segmented. Further, spine detection is performed manually; the user clicks on each spine, and the tool computes the morphological features and performs classification using a rule based approach. As can be seen from the results presented in Table 1 performance of 2dSpAn is even worse than our morphological features based approach (Ghani et al., 2015). Additionally, our shape and appearance features based approach performs almost twice as well as 2dSpAn.

We compare the performance of our approach using three classifiers: KDE, support vector machines (SVM) and Neural Networks (NN). We used a linear kernel for SVM and a 2-layer back-propagation trained feed-forward network with $\frac{No.\ of\ features + No.\ of\ Classes}{2}$ nodes in each layer for Neural Network based classification. We compare shape, appearance, and morphological feature extraction schemes for all three classifiers using 10 fold cross validation. Classification results are presented in Table 1.

As we can see from Table 1, the proposed shape and appearance based feature extraction techniques result in higher classification accuracy for all classifiers with respect to commonly used morphological features (Rodriguez et al., 2008; Koh et al., 2002; Ghani et al., 2015; Basu et al., 2016) on all datasets. It is also clear from presented results that HOG based appearance features perform slightly better than DNSM features. Combining DNSM and HOG performs slightly better in some cases. Further applying feature selection on DNSM + HOG results in higher accuracy in some cases. Another conclusion to draw from Table 1 is that our proposed shape and appearance features combined with Neural Network outperforms other classification methods. We demonstrate the usefulness of advanced machine learning classification approaches, KDE, SVM, and NN, for classification of dendritic spines and demonstrate their advantages over classical rule-based approaches. Additionally, our KDE based framework provides the statistical description in terms of the shape and appearance features.

4.1. Likelihood-ratio space analysis

As discussed earlier, whether to view spines as belonging to distinct shape classes or to model them through a continuum of shape variations is still an open question. Since our KDE based classification approach gives the likelihood of a spine being member of mushroom (l_m), stubby (l_s), and thin (l_t) classes, it can be used to examine this question in a principled manner. We computed the histogram of likelihood ratios ($\mathcal{L}_s$ and $\mathcal{L}_t$), as given in Fig. 6 and analyzed whether we see three distinct modes or a continuum of

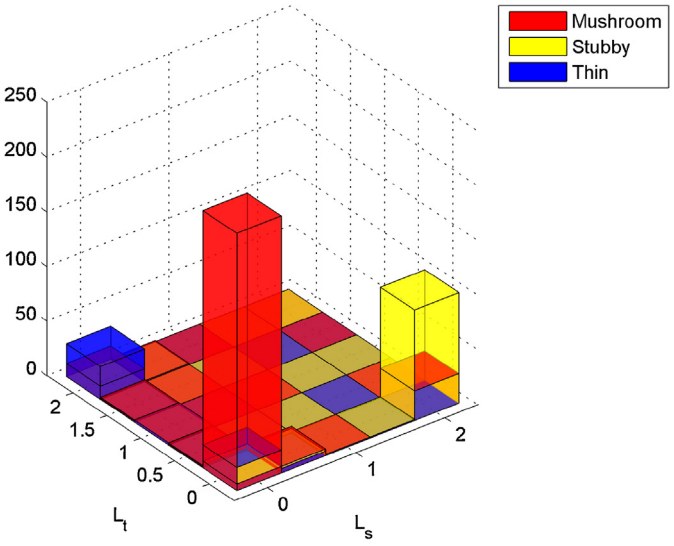

Fig. 6. 2D likelihood ratio space produced using DNSM + HOG + InfoGain on DatasetA. We have added transparency in the histogram for improved visualization. We can see three peaks; however, the samples of each shape are distributed all over. With the aid of transparency, we can see different shape samples spread over the grid produced as a mixture of different colors such as red and yellow, yellow and blue, etc.

Table 2
Two-sample two-dimensional Kolmogorov–Smirnov test results for different class separation problems. We use the null hypothesis that each pair of distributions has the same mean, which is rejected in all cases, supporting the existence of distinct shape classes.

Test	p-value	Rejected/accepted
Mushroom vs. stubby	1.49×10^{-43}	Rejected
Mushroom vs. thin	3.05×10^{-19}	Rejected
Stubby vs. thin	1.54×10^{-25}	Rejected

shapes. It is evident from the presented histogram that we see three peaks, however the samples of three classes can be found all over the grid. One might argue that there are three classes, mushroom, stubby, and thin, but there is a significant overlap between their distributions. To analyze the statistical significance of the hypothesis that these spine classes have distinct means in the space of likelihoods, we performed multi-variate analysis of variance (MANOVA) with the null hypothesis that all class distributions have the same mean. Since we have two dependent variables, $\mathcal{L}_s$ and $\mathcal{L}_t$, and three classes, MANOVA is a fair choice for statistical significance analysis. We applied MANOVA on our data and found that it rejects the null hypothesis at $\alpha = 0.05$ significance level. MANOVA rejects the existence of a continuum of shape variations. Further, we apply post-hoc tests to analyze the individual class separability using a two-sample bi-variate Kolmogorov–Smirnov test (Peacock, 1983) with the null hypothesis that each pair of distributions has the same mean. Here, we perform three tests to analyze mushroom vs. stubby, mushroom vs. thin, and stubby vs. thin class separations. The test results are given in Table 2. The null hypothesis is rejected in all cases supporting the argument for the existence of distinct classes. It provides us an insight that class distributions have different means, meaning that there exist three distinct classes in our dataset. Such low p-value strongly supports the significance of our analysis. However, these results are dependent on how the experiment has been performed and the particular data set obtained. While our findings apply to this particular data set, the analysis tools we have proposed would be useful in similar spine shape analysis problems.[5]

If we treat this problem as a classification task, the best performance (assuming equal priors and the probability of error as the decision criterion) can be achieved by thresholding in the 2D likelihood ratio space as illustrated in Fig. 5 to perform classification. However, classifying the spines lying around these decision boundaries is a difficult decision since values of $\mathcal{L}_s$ and $\mathcal{L}_t$ are very close in such cases. Our KDE based framework provides a principled approach to handle such spines. If values of $\mathcal{L}_s$ and $\mathcal{L}_t$ are not very different, one might use the help of neuroscientists to investigate the spines and make a decision manually. Further analysis may also include 3D image evaluation of the spines whose likelihoods for different classes are very close.

5. Conclusion

We have considered the problem of dendritic spine shape analysis and proposed a framework for shape and appearance-based feature extraction and statistically-based classification from 2PLSM images of neurons. This study provides a new direction to researchers working in this domain. We investigated the use of a shape feature extraction technique, DNSM, and an appearance feature extraction technique, HOG. We begin with intensity images and perform segmentation using DNSM, which is a parametric shape model and provides DNSM parameters along with segmentation. We use DNSM parameters of resulting segmented images as shape features. Further, we compute HOG based appearance features from intensity images. We perform different experiments by combining shape and appearance features and compare performance of our proposed feature extraction approach to three morphological feature based approaches reported in the literature.

We compare classification performance using KDE, SVM, and NN classifiers, and find that our approach outperforms three state-of-the-art morphological features based approaches. Our shape and appearance features combined with advanced machine learning classifiers outperforms existing spine feature extraction and classification methods. Our feature extraction methods are generic in the sense that they can be combined with other state-of-the-art classifiers. Additionally, our KDE based feature analysis approach is useful not only to perform classification but also to study the statistical distribution of spine classes to contribute towards questions of identifiability of distinct spine classes. We present a histogram of likelihood ratios which provides an insight into the challenging nature of the spine shape analysis problem. Likelihood ratio space shows three peaks but samples of all classes are spread all over. Further, we apply a MANOVA test to check the statistical significance of our analysis and which supports the idea of distinct shape classes on the spine data used in this paper. While our conclusion applies to this particular data set, the analysis tools we have proposed would be useful in similar spine shape analysis problems. This work is based on MIP 2D spine images, however, we expect that analysis performed on 3D data would provide better performance in principle. Many pieces of our approach can be extended to 3D in a straightforward way and we are currently working on to extend the tools for analysis of 3D data.

We have used a KDE based approach for classification, however, one could use the KDE framework to output continuous probabilistic scores rather than class assignments. Another interesting extension of this work could be to propose a new shape representation consisting of shape primitives that can compactly represent spine parts such as head and neck, which could seamlessly produce biologically meaningful features such as neck length. Furthermore, we analyzed the question of continuum of shape variations, which should be further investigated on more datasets using our framework which could potentially contribute to this on-going debate. On the technical side, tools could be developed to study spine shapes in an unsupervised fashion, which would reduce subjective biases introduced due to the supervised nature of classification based analysis. Another challenge is that due to the subjective nature of class assignment by human experts, the process can be uncertain. In such cases, one could provide a confidence level during the label assignment process, so if a classification framework makes a mistake for cases when even a human expert is unsure, it should not be considered an error.

[5] https://github.com/mughanibu/Non_Parametric_Kernel_Density_Estimation.

Acknowledgements

This work has been supported by the Scientific and Technological Research Council of Turkey (TUBITAK) under Grant 113E603, by TUBITAK-2218 Fellowship for Postdoctoral Researchers, and by a TUBITAK-2221 Fellowship for Visiting Scientists and Scientists on Sabbatical Leave.

References

Arellano, J.I., Benavides-Piccione, R., DeFelipe, J., Yuste, R., 2007. Ultrastructure of dendritic spines: correlation between synaptic and spine morphologies. Frontiers Neurisci. 1 (1), 131–143.
Atherton, T., Kerbyson, D., 1999. Size invariant circle detection. Image Vis. Comput. 17 (11), 795–803.

Bartol, T.M., Bromer, C., Kinney, J.P., Chirillo, M.A., Bourne, J.N., Harris, K.M., Sejnowski, T.J., 2015. Hippocampal spine head sizes are highly precise. bioRxiv, 1–14.
Basu, S., Plewczynski, D., Saha, S., Roszkowska, M., Magnowska, M., Baczynska, E., Wlodarczyk, J., 2016. 2dspan: semiautomated 2-D segmentation, classification and analysis of hippocampal dendritic spine plasticity. Bioinformatics 32 (16), 2490–2498.
Chang, F., Greenough, W.T., 1984. Transient and enduring morphological correlates of synaptic activity and efficacy change in the rat hippocampal slice. Brain Res. 309, 35–46.
Cover, T.M., Thomas, J.A., 1991. Elements of Information Theory. Wiley.
Dalal, N., Triggs, B., 2005. Histograms of oriented gradients for human detection. In: IEEE Computer Society Conference on Computer Vision and Pattern Recognition, 2005. CVPR 2005, vol. 1, IEEE, pp. 886–893.
Erdil, E., Argunsah, A.O., Tasdizen, T., Unay, D., Cetin, M., 2015. A joint classification and segmentation approach for dendritic spine segmentation in 2-photon microscopy images. In: IEEE 12th International Symposium on Biomedical Imaging (ISBI), IEEE, pp. 797–800.
Ghani, M.U., Kanik, S.D., Argunsah, A.O., Tasdizen, T., Unay, D., Cetin, M., 2015. Dendritic spine shape classification from two-photon microscopy images. In: IEEE Signal Processing and Communications Applications (SIU).
Ghani, M.U., Mesadi, F., Kanik, S.D., Argunsah, A.O., Israely, I., Unay, D., Tasdizen, T., Cetin, M., 2016. Dendritic spine shape analysis using disjunctive normal shape models. In: IEEE 13th International Symposium on Biomedical Imaging (ISBI).
Ghani, M.U., Argunsah, A.O., Israely, I., Unay, D., Tasdizen, T., Cetin, M., 2016. On comparison of manifold learning techniques for dendritic spine classification. In: IEEE 13th International Symposium on Biomedical Imaging (ISBI).
Ghani, M.U., Erdil, E., Kanik, S.D., Argunsah, A.O., Hobbiss, A.F., Israely, I., Unay, D., Tasdizen, T., Cetin, M., 2016. Dendritic Spine Shape Analysis: A Clustering Perspective. Springer International Publishing.
Govindarajan, A., Israely, I., Huang, S.-Y., Tonegawa, S., 2011. The dendritic branch is the preferred integrative unit for protein synthesis-dependent LTP. Neuron 69 (1), 132–146.
Hall, M.A., Ph.D. thesis 1999. Correlation-based feature selection for machine learning. The University of Waikato.
Harris, K.M., Jensen, F.E., Tsao, B., 1992. Three-dimensional structure of dendritic spines and synapses in rat hippocampus (ca1) at postnatal day 15 and adult ages: implications for the maturation of synaptic physiology and long-term potentiation. J. Neurosci. 12 (7), 2685–2705 (published erratum appears in J. Neurosci. 12 (8) (1992): following table of contents).
Harris, K.M., 1999. Structure, development, and plasticity of dendritic spines. Curr. Opin. Neurobiol. 9 (3), 343–348.
Harvey, C.D., Svoboda, K., 2007. Locally dynamic synaptic learning rules in pyramidal neuron dendrites. Nature 450 (7173), 1195–1200.
Kim, J., Cetin, M., Willsky, A.S., 2007. Nonparametric shape priors for active contour-based image segmentation. Signal Process. 87 (12), 3021–3044.
Koh, I.Y., Lindquist, W.B., Zito, K., Nimchinsky, E.A., Svoboda, K., 2002. An image analysis algorithm for dendritic spines. Neural Comput. 14 (6), 1283–1310.
Lippman, J., Dunaevsky, A., 2005. Dendritic spine morphogenesis and plasticity. J. Neurobiol. 64 (1), 47–57.
Lipson, A., Lipson, S.G., Lipson, H., 2010. Optical Physics. Cambridge University Press.
Matsuzaki, M., Honkura, N., Ellis-Davies, G.C., Kasai, H., 2004. Structural basis of long-term potentiation in single dendritic spines. Nature 429 (6993), 761–766.
Mesadi, F., Cetin, M., Tasdizen, T.,2015. Disjunctive normal shape and appearance priors with applications to image segmentation. In: Medical Image Computing and Computer-Assisted Intervention–MICCAI 2015. Springer, pp. 703–710.
Parnass, Z., Tashiro, A., Yuste, R., 2000. Analysis of spine morphological plasticity in developing hippocampal pyramidal neurons. Hippocampus 10 (5), 561–568.
Peacock, J., 1983. Two-dimensional goodness-of-fit testing in astronomy. Monthly Notices of the Royal Astronomical Society 202 (3), 615–627.
Peters, A., Kaiserman-Abramof, I.R., 1970. The small pyramidal neuron of the rat cerebral cortex. the perikaryon, dendrites and spines. Am. J. Anat. 127, 321–356.
Ramesh, N., Mesadi, F., Cetin, M., Tasdizen, T., 2015. Disjunctive normal shape models. In: 12th IEEE International Symposium on Biomedical Imaging (ISBI), pp. 1535–1539, http://dx.doi.org/10.1109/ISBI.2015.7164170.
Richard, L., Burden, J., 1988. Douglas Faires, Numerical Analysis.
Rodriguez, A., Ehlenberger, D.B., Dickstein, D.L., Hof, P.R., Wearne, S.L., 2008. Automated three-dimensional detection and shape classification of dendritic spines from fluorescence microscopy images. PLoS One 3 (4), 1–12.
Ruszczycki, B., Szepesi, Z., Wilczynski, G.M., Bijata, M., Kalita, K., Kaczmarek, L., Wlodarczyk, J., 2012. Sampling issues in quantitative analysis of dendritic spines morphology. BMC Bioinform. 13, 213.
Shi, P., Zhou, X., Li, Q., Baron, M., Teylan, M.A., Kim, Y., Wong, S.T., 2009. Online three-dimensional dendritic spines mophological classification based on semi-supervised learning. In: ISBI'09 IEEE International Symposium on Biomedical Imaging: From Nano to Macro, pp. 1019–1022.
So, P.T., Dong, C.Y., Masters, B.R., Berland, K.M., 2000. Two-photon excitation fluorescence microscopy. Annu. Rev. Biomed. Eng. 2 (1), 399–429.
Son, J., Song, S., Lee, S., Chang, S., Kim, M., 2011. Morphological change tracking of dendritic spines based on structural features. J. Microsc. 241 (3), 261–272.
Spacek, J., Hartmann, M., 1983. Three-dimensional analysis of dendritic spines. I. Quantitative observations related to dendritic spine and synaptic morphology in cerebral and cerebellar cortices. Anat. Embryol. 167, 289–310.
Tenenbaum, J.B., de Silva, V., Langford, J.C., 2000. A global geometric framework for nonlinear dimensionality reduction. Science 290 (5500), 2319–2323.
Tonnesen, J., Katona, G., Rózsa, J., Nagerl, U., et al., 2014. Spine neck plasticity regulates compartmentalization of synapses. Nat. Neurosci. 17 (5), 678–685.
Wallace, W., Bear, M.F., 2004. A morphological correlate of synaptic scaling in visual cortex. J. Neurosci. 24 (31), 6928–6938.
Wallis, J., Miller, T.R., Lerner, C., Kleerup, E., 1989. Three-dimensional display in nuclear medicine. IEEE Trans. Med. Imaging 8 (4), 230–297.
Whitlock, J.R., Heynen, A.J., Shuler, M.G., Bear, M.F., 2006. Learning induces long-term potentiation in the hippocampus. Science 313 (5790), 1093–1097.
Xu, X., Wong, S., 2006. Optical microscopic image processing of dendritic spines morphology. IEEE Signal Process. Mag. 23 (4), 132–135.
Yuste, R.B.T., 2001. Morphological changes in dendritic spines associated with long-term synaptic plasticity. Annu. Rev. Neurosci. 24, 1071–1089.
Yuste, R., 2010. Dendritic Spines. MIT Press.